

Automated Atlas Integration and Interactive Three-Dimensional Visualization Tools for Planning and Guidance in Functional Neurosurgery

Philippe St-Jean, Abbas F. Sadikot, Louis Collins, Diego Clonda, Reza Kasrai, Alan C. Evans, and Terry M. Peters,* *Senior Member, IEEE*

Abstract—Many critical functionally distinct subcortical structures are not distinguishable on anatomical magnetic resonance imaging (MRI) scans. In order to provide the neurosurgeon with this missing information, a deformable volumetric atlas of the basal ganglia and thalamus has been created from the Schaltenbrand and Wahren atlas of cryogenic slices. The volumetric atlas can be automatically deformed to an individual patient's MRI. To facilitate the clinical use of the atlas, a visualization platform has been developed for preoperative and intraoperative use which permits manipulation of the merged atlas and MRI data sets in two- and three-dimensional views. The platform includes graphical tools which allow the visualization of projections of a leukotome and other surgical tools with respect to the atlas data, as well as preregistered images from any other imaging modality. In addition, a graphical interface has been designed to create custom virtual lesions using computer models of neurosurgical tools for intraoperative planning. To date this system has been employed as an adjunct to over 30 functional neurosurgical cases including surgery for movement disorders.

Index Terms—Atlas-based guidance, image-guided neurosurgery, movement disorders, Parkinson's disease, thalamus, three-dimensional (3-D) visualization.

I. INTRODUCTION

A. Clinical Motivation

STEREOTACTIC neurosurgery in critical brain areas requires excellent appreciation of boundaries of function-

Manuscript received February 23, 1998; revised June 12, 1998. The work of A. F. Sadikot, A. C. Evans, and T. M. Peters was supported by operating grants from the Medical Research Council of Canada (MRC). The work of T. M. Peters was also supported by the Natural Sciences and Engineering Research Council of Canada (NSERC). The work of P. St-Jean, D. Clonda, and R. Kasrai was supported by NSERC post-graduate studentships. The Associate Editor responsible for coordinating the review of this paper and recommending its publication was M. Viergever. *Asterisk indicates corresponding author.*

P. St-Jean and D. Clonda were with the McConnell Brain Imaging Centre and the Department of Neurology and Neurosurgery, Montréal Neurological Institute and Hospital, McGill University, Montréal, P.Q., Canada. They are now with the Department of Physics, Université de Montréal, Montréal, P.Q., Canada.

A. F. Sadikot is with the Department of Neurology and Neurosurgery, Montréal Neurological Institute and Hospital, McGill University, Montréal, P.Q., Canada.

L. Collins, R. Kasrai and A. C. Evans are with McConnell Brain Imaging Centre and the Department of Neurology and Neurosurgery, Montréal Neurological Institute and Hospital, McGill University, Montréal, P.Q., Canada.

*T. M. Peters was with the McConnell Brain Imaging Centre, Montréal Neurological Institute and Hospital, McGill University, Montréal, P.Q., Canada. He is now with the Robarts Research Institute, London ON, Canada.

Publisher Item Identifier S 0278-0062(98)08748-5.

ally distinct regions that are not delineated adequately by anatomical imaging methods. For stereotactic guidance in such regions, surgeons have used atlases sectioned in well-defined planes and processed histologically to reveal distinct nuclei within structures such as the thalamus and the basal ganglia. The increasing use of functional stereotactic neurosurgery for disorders such as Parkinson's disease and epilepsy, motivated us to develop an interactive visualization platform to facilitate these procedures. Its facilities include automatic integration of a standard brain atlas into the patient's volumetric magnetic resonance imaging (MRI) space, interactive display of stereotactic instruments in the integrated atlas-MRI space, and lesion-modeling with respect to the target nuclei. The platform was initially developed for surgical treatment of Parkinson's disease, but has wide-ranging implications for many procedures in critical brain areas involving frameless or frame-based stereotactic methods.

Symptomatic Parkinson's disease manifests in a variety of ways including tremor, rigidity, bradykinesia, and impaired gait. Pharmacological treatments are used initially to improve many of these symptoms, but medically intractable cases are often referred for stereotactic neurosurgical procedures in deep brain areas. Parkinsonian patients suffering from significant tremors can benefit from a lesion created in the thalamus (thalamotomy) [1], while lesions in the globus pallidus (pallidotomy) are usually performed when the patient suffers from rigidity or drug-induced abnormal movements. The probability of worthwhile relief of symptoms in these patients is around 80%. Currently at the Montreal Neurological Institute (MNI), the target for thalamotomy is the nucleus ventralis intermedius (Vim), while the target for pallidotomy is within the medial part of the globus pallidus (GPM).

B. The Stereotactic Frame

Since these operations involve deep-brain structures, image-guidance is required to delineate the target structure and its surrounding area, and so a stereotactic device is attached to the patient's head as a reference frame. The frame may then be visualized with respect to the patient's brain using a variety of imaging methods. An arc system mounted on the frame provides support and orientation for tools during the neurosurgical procedure (Fig. 1), and a small burr-hole in the skull is used to introduce instruments en route to deep target areas. Once the orientation of the arc is fixed with respect

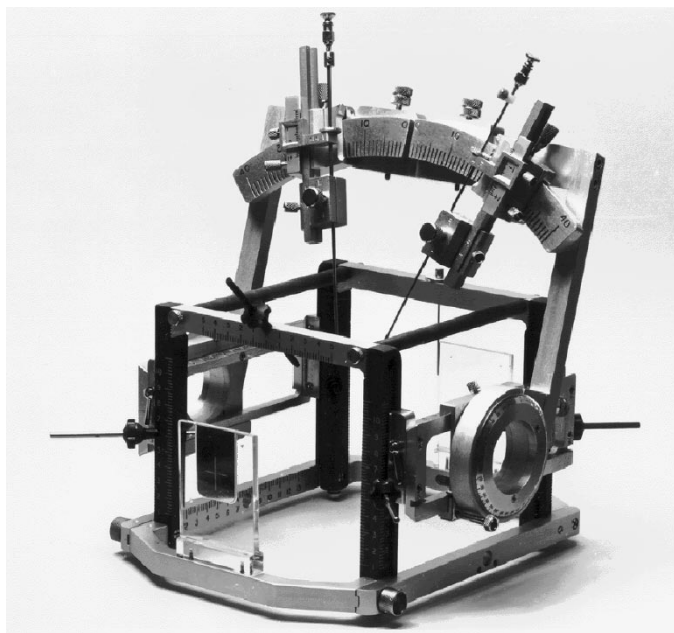


Fig. 1. Arc system mounted on the stereotactic frame. As an example, two biopsy needles are attached to the arc system.

to the frame, the loci of positions of the tool-holder lie on a spherical surface. In this configuration, when the tool is set at the zero-offset position with respect to the tool-holder, the tip of the tool is exactly at the center of the sphere which is localized at the target position [2].

C. Conventional Imaging Modalities for Thalamotomy and Pallidotomy

At the MNI, the standard procedure for performing stereotactic localization of the targets makes use of multimodality imaging, including ventriculography (Fig. 2), computed tomography (CT), digital subtraction angiography (DSA) and MRI [3]. Even though landmarks such as the midplane (the sagittal cut between the two hemispheres) and the AC-PC plane¹ can be easily localized on ventriculograms, the positions of the target structures relative to such landmarks are not necessarily constant between patients due to normal anatomical variability.

Anatomical structures are partly delineated by boundaries between gray and white matter. Whereas CT scans show some contrast between these tissues, MRI is clearly superior in distinguishing gray-white matter boundaries. However, MRI cannot differentiate between functionally distinct structures within gray matter, such as the Vim and its neighboring thalamic nuclei. We generally employ a ventriculogram in conjunction with three-dimensional (3-D) MRI for stereotactic localization. The stereotactic ventriculogram delineates the boundaries of cerebrospinal fluid-filled spaces (e.g., the third ventricle), which are close to target structures such as the thalamus and globus pallidus. Measurements made on ventriculography can be correlated with those derived from MRI,

¹The AC-PC plane contains the line between the anterior and posterior commissure (AC and PC) points and is perpendicular to the plane between the two hemispheres (the midplane).

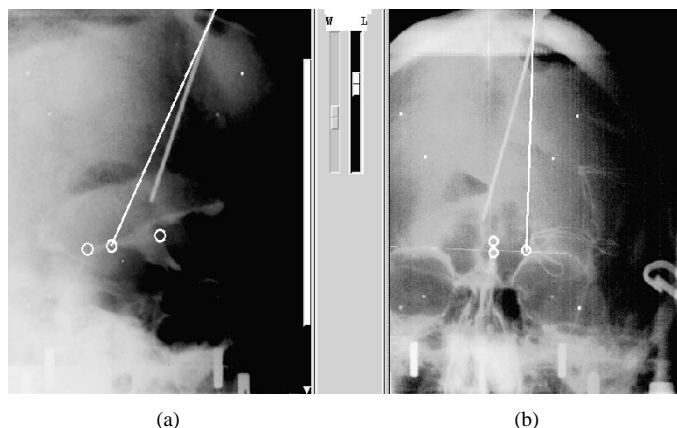


Fig. 2. Ventriculograms. (a) Lateral and (b) antero-posterior ventriculograms with the AC, PC, and target points identified.

and this allows for correction of possible distortion due to magnetic field inhomogeneity [4]. MRI is nevertheless the modality which provides most of the information relating to the anatomy of the thalamus, basal ganglia, and neighboring structures, and is used for atlas integration. It has been demonstrated that judicious use of a combined CT-MR imaging technique, in conjunction with microelectrode recording, may obviate the need for the stereotactic ventriculography [5]. However, by comparing it with intraoperative stereotactic skull X rays, we find the ventriculogram is also very useful for intraoperative confirmation of the position of surgical tools.

D. Stereotactic Neurosurgical Tools

The tools commonly employed in Parkinson's surgery at the MNI are the leukotome [6] [Fig. 3(a)] for creating the lesions, and a monopolar electrical stimulator [Fig. 3(b)] for eliciting responses from the patient prior to lesion generation. To address interpatient anatomical variability, physiological verification of the stereotactic position of target structures and peri-target areas is performed by electrical stimulation. A stimulating electrode is inserted into the patient's brain through the same burr-hole used for the injection of the ventriculography contrast agent. The stimulator consists of an insulated conducting wire exposed at its tip, which protrudes in a well-defined curve from the distal end of a metallic shaft. Compared to the straight electrode, this curvilinear geometry allows the surgeon to physiologically stimulate larger brain volumes with fewer passages from the brain surface to the target, thus reducing the risk of hemorrhage. The probe may be protracted in different directions searching a well-defined volume, and a single pass to the target area often yields the required physiological confirmation of anatomical localization. A calibrated screw with a millimeter scale at the proximal end of the stimulator controls the extent of protrusion of the electrode from the tip of the shaft. The stimulator tip currently used at the MNI extends a maximum of 14 mm from the end of the shaft. The neurosurgeon stimulates various regions of the thalamus or globus pallidus, and important white matter structures such as the internal capsule or optic tract. The resulting sensory, motor, or visual responses obtained from electrical stimulation, allow the neurosurgeon to confirm the

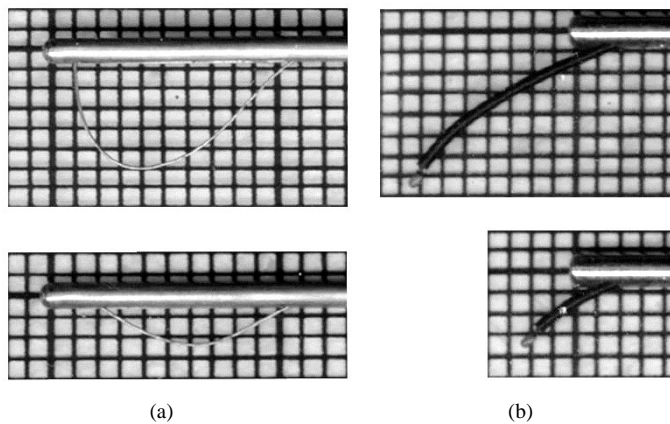


Fig. 3. The leukotome (a), and the stimulator (b) each represented at two different protrusion setting.

position of the target relative to critical surrounding areas [7]. Once sufficient information about the position of the important deep brain structures has been obtained, the neurosurgeon can proceed to perform a tailored lesion within the Vim or the GPM.

The leukotome consists of a thin metallic wire which protrudes from a shaft (similar to the stimulator) in the form of a loop, and acts like a knife when the tool is rotated around its axis [Fig. 3(a)] [6]. The MNI leukotome has a calibrated screw with a scale at the proximal extremity of the shaft, which allows the neurosurgeon to control the extent of loop protrusion in a graded fashion. The leukotome loop extends to a maximum distance of 7 mm from the shaft. The main advantage of the leukotome over other tools resides in its ability to create tailored lesions conforming to the shape of the target structure. While other methods are usually limited to spherical lesions with indistinct boundaries, the leukotome allows for predefined lesions that can be geometrically adapted to the target volume. Custom lesion shapes can be achieved by varying the extent of loop protrusion in different sectors as the tool is rotated. We note here that the leukotome is just one of several tools available for stereotactic lesioning. Other groups employ radio-frequency (RF) heating to ablate brain tissue [8]. As an alternative to lesioning, chronic electrical stimulation of the target nucleus has also been described [9].

Although conventional techniques are effective, standard imaging modalities do not allow functionally distinct deep brain structures to be distinguished. This shortcoming inherently precludes visualization of patient-specific geometry of target subnuclei within the thalamus or basal ganglia structures such as the pallidal segments or subthalamic nucleus. Furthermore, it is difficult to mentally reconstruct the 3-D relationship of these deep structures and intraoperative surgical tools with accuracy. It is particularly important to visualize the configuration of the final lesion with respect to critical deep brain structures in order to conform to the target area and prevent unnecessary lesions in neighboring nuclei or white matter tracts. We developed an interactive atlas-based 3-D intraoperative visualization platform (see Section II-D), in order to provide interactive visual feedback to the neurosurgeon, and to increase the accuracy of target localization.

II. MATERIALS AND METHODS

A. Atlases and Automatic Labeling of Deep Brain Structures

Various atlases of the human brain serve as references for clinicians and researchers interested in stereotactic localization of subnuclei within deep brain structures [10]–[12]. However, these atlas structures differ in size and geometry from those of any given patient's brain. In addition, during surgery, it may be difficult to appreciate the orientation of the patient's brain and the trajectory of neurosurgical tools with respect to the slices presented in the atlases. Since no currently available *in-vivo* imaging modality provides sufficient image contrast between target structures, the solution implemented here was to enhance the information already available from routine MRI scans. The Schaltenbrand and Wahren atlas [12] is one of the principal anatomical references for neurosurgeons performing thalamotomies and pallidotomies.² While computer-based atlases exist, [13], [14] none of these were available to us in the appropriate electronic form to serve as a basis for this project. Early work on the use of digitized atlases to guide thalamotomy surgery was reported as early as 1972 by Bertrand and Thompson [15], [16], who correlated atlas slices with ventriculograms. The aim of this present work is to incorporate the precise contours of an anatomical atlas of deep brain structures with an individual patient's 3-D MRI scan. Such an atlas must be volumetric, deformable, and capable of being accurately registered to the patient's deep-brain anatomy.

The Schaltenbrand and Wahren atlas gathers together many different data sets, three of which are of interest: the coronal (plates 35–40 of the atlas), sagittal (plates 41–51) and transverse (plates 52–57) cryogenic slices of human cadaver brains. Each of these three data sets consists of a series of micro-thin cryotome slices, which were stained to discriminate between structures presenting different cytoarchitecture. The slices are not necessarily contiguous in space, being separated by distances varying from 0.5–3.0 mm. The atlas consists of photographs of these slices with superimposed alignment grids and outlines of anatomical regions delineated on acetate overlay sheets (Fig. 4).

A single atlas is only applicable to the brain from which it was derived, presenting the problem of intersubject variability when attempting application to individual subjects. Our objective was to overcome this limitation by creating a volumetric digital atlas based on these two-dimensional (2-D) slices, that could be deformed to fit the deep-brain structures of any individual. Since the most detailed anatomical information from these data sets was available in the transverse plane, this set was used as a basis for the construction of the 3-D atlas. In this series, over one hundred structures are outlined, but for our purposes, the volumetric atlas was limited to 16 regions of interest relevant to surgical procedures involving the thalamus, subthalamic nucleus or globus pallidus. The steps involved in the creation of the volumetric version of the Schaltenbrand and Wahren atlas were as follows.

²The sagittal and axial sets come respectively from the left and right hemispheres of the same cadaver brain (number LXXVIII). The coronal set comes from another brain (LXVIII). (Roman numerals refer to cadaver brains used in the construction of the Schaltenbrand and Wahren Atlas.)

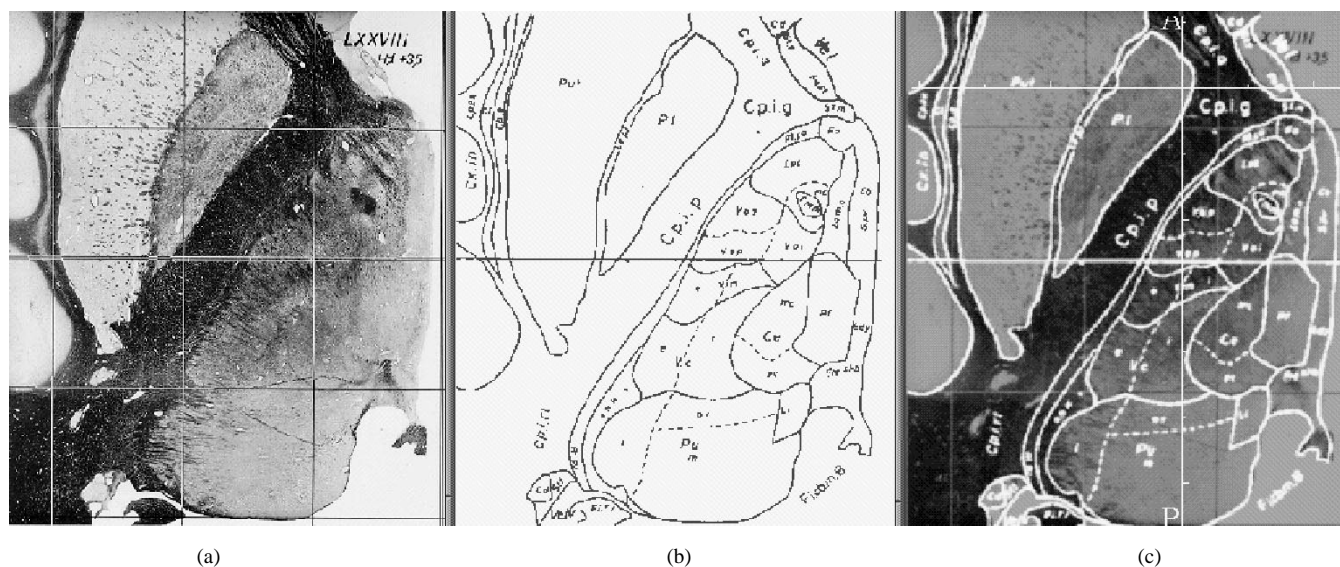


Fig. 4. An axial slice from the Schaltenbrand and Wahren transverse series: (a) stained histologic slice, (b) transparent overlay contours, and (c) superimposition of the two. (Reproduced with permission of Georg Thieme Verlag).

- digitizing both the cryotome slices and the transparent contour overlays;
- stacking and aligning (concatenating) the individual slices into a 3-D data set;
- extracting the 2-D contours (from the transparent overlay) in a vector format;
- performing an interpolation of the 2-D contours, using Hermite polynomials, to achieve a 3-D representation of the structures.

Scanning of the cryogenic slices and acetate overlays was performed using a standard flat-bed image scanner. The (4×) magnified images were digitized with a resolution of 72 dots per inch, which yielded a pixel spacing of approximately 0.1 mm. The slices were initially aligned using the grid system already present in the Schaltenbrand and Wahren atlas, and software was created to render the stack of slices into a volumetric data set. Voxels in the 3-D volume for which no data were present in the atlas, were initially set to zero. We note that the grid structure present in the atlas was placed on the cryotome images subsequent to photography, and so even precise alignment with respect to the grid is no guarantee that the underlying slices were not themselves distorted during the slicing process. However, our methodology for matching the slices with the model 3-D MRI volume (described later) automatically corrects for such distortions.

When visualized in a tri-planar display,³ this preliminary volumetric data set presents either structure-contours or a completely black image in the transverse view, while only a set of sparse dots or lines is seen in the other two views. In order to convert this data set into a full 3-D volume, an interpolation operation between these axial slices was performed using spline parameterization of the 3-D curves with Hermite cubic interpolation as outlined by Foley *et al.* [17]. The interiors of these 16 regions were then assigned numerical values to

create a volumetric version of the atlas with an isotropic voxel dimension of 0.5-mm along each axis.

B. The Automatic Nonlinear Image Matching and Anatomical Labeling (ANIMAL) Algorithm

In the context of this paper, we use the term “linear” to describe any transformation that can be accommodated using a constrained affine transform (disallowing reflection and skew). “Nonlinear” refers to transformations whose characteristics change between locations in the image. Computerized volumetric versions of stereotactic atlases that allow only linear deformation, although useful, are still somewhat limited from a neurosurgical point of view. Even when such atlases are translated, rotated and scaled to fit the region of the thalamus and basal ganglia as seen on the patient’s MRI (using a Talairach-like constrained affine transformation [11]), normal intersubject anatomical variability and possible anatomy-deforming pathology prevent the atlas overlay from being sufficiently accurate for surgical navigation purposes. As a result, the atlas needs to be deformed locally in order to take into account the patient’s anatomy. The objective of this part of the project was to develop a methodology to create a customized version of the Schaltenbrand and Wahren atlas for each patient on a routine basis, in a completely automatic fashion, so that no manual intervention is required.

The ANIMAL algorithm [18], was designed to compute a nonlinear transformation to register one MRI (the patient image) to a second pre-labeled target MRI that serves as a canonical atlas. Segmentation of the patient MRI is achieved by using the inverse of this transformation to warp the canonical atlas back onto the patient’s 3-D MR image. The registration procedure operates in two stages. In the first step, ANIMAL computes a constrained affine transformation, optimizing the three translations, three rotations, and three (positive) scales required to register the two volumes. In the second step, ANIMAL deforms the first MRI volume to match the second.

³A set of three orthogonal planes (usually sagittal, axial, and coronal), the intersection of which is the point of interest.

It builds up the 3-D nonlinear deformation field in a piecewise linear fashion, fitting cubical neighborhoods in sequence. Each data cube in one volume is translated to achieve an optimal match within the other volume. Cubes are arranged in a 3-D grid to fill the volume and each cube moves within a range defined by the grid-spacing. The algorithm is applied in a multiscale hierarchy. At each step, the image volumes are preconvolved with a 3-D Gaussian kernel, while the extent of the blurring kernel and cube sizes are reduced after each stage. Initial fits are obtained rapidly since at lower scales, only gross distortions are considered, but later iterations at finer scales accommodate local differences at the price of increasing computational burden. Segmentation is finally achieved by transforming the canonical atlas labels associated with the model MRI onto the patient's MRI, using the inverse of the 3-D deformation field.

Since ANIMAL requires both the original and target volumes to be MR images, the atlas cannot be warped directly onto the patient's MRI data.

Therefore, it is necessary to perform an intermediate step by defining the Schaltenbrand and Wahren atlas with respect to a single MRI volume that will then serve as a link between the atlas and the patient's MRI. Once a suitable intermediate MRI data set is selected, the atlas must be registered to it. This time consuming operation involving manual tagging of atlas structure to the model MRI needs to occur only once. When applied clinically to individual patients, atlas registration occurs automatically using the ANIMAL algorithm.

C. The Model MRI Data Set

While any 3-D MRI volume could be used in ANIMAL, we selected a model MRI data set that has been created from an average of 27 T1-weighted modulus volumetric MRI scans of the same individual, collected over a period of several months (Fig. 5) [19]. These images were registered to sub-voxel accuracy and averaged together to increase the signal-to-noise ratio (SNR). While the statistical distribution of the noise in a modulus MRI image is, in general, Rician, in regions of high intensity it is approximately Gaussian [20]. The measured SNR improvement (computed by measuring the noise standard-deviation in similar white-matter regions of both single and averaged images) was 5.1, consistent with the assumption of Gaussian noise statistics.

Three-dimensional thin-plate spline interpolation based on the approach of Bookstein [21] was used to register the volumetric version of the Schaltenbrand and Wahren atlas onto the model MRI volume, since it defines a smooth nonlinear transformation based on a set of homologous point pairs. In this case, each pair of points consisted of corresponding anatomical landmarks: one point from the model brain MRI data set and the other from the atlas. A neuroanatomist identified 250 homologous landmarks (Fig. 6) using a program "REGISTER".⁴ This system allows independent, simultaneous, tri-planar (sagittal, coronal, and transverse) viewing of both MRI and atlas volumes in 2-D slice windows with arbitrary pan and zoom, permitting the user to accurately identify

⁴ Available via anonymous ftp site: <ftp.mni.mcgill.ca/pub/register+Display>.

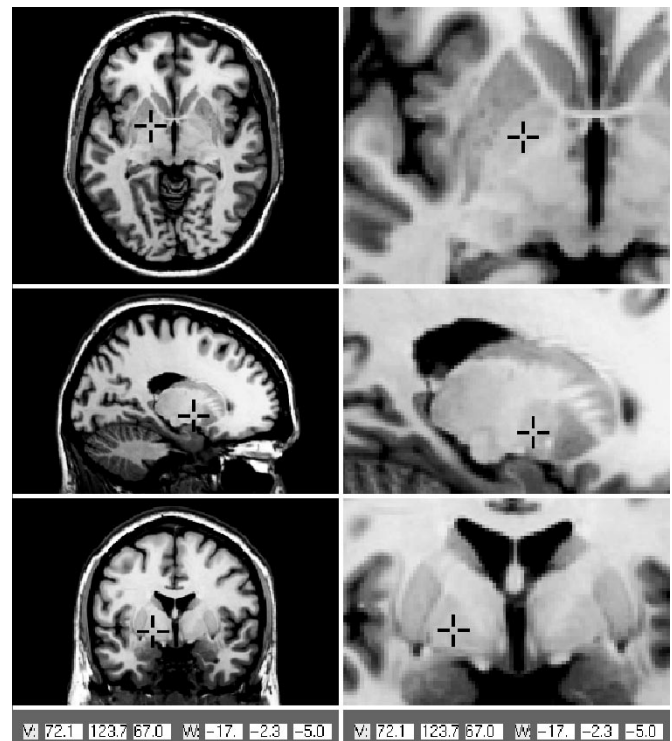


Fig. 5. The MRI model data set: axial, sagittal, and coronal cuts (top to bottom), with corresponding detail views (right series).

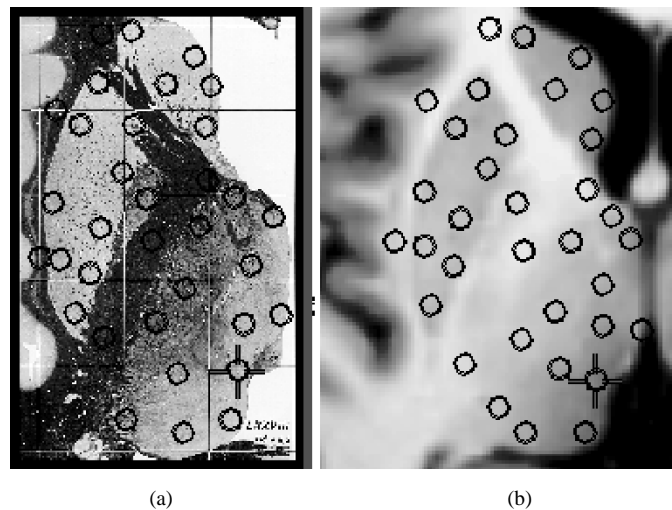


Fig. 6. Example of corresponding tag points between (a) the atlas and (b) the MRI model.

landmark points in three dimensions. Thus, the matching of the homologous point pairs, which was greatly facilitated by using the high SNR model MRI volume, was a truly 3-D operation. After the identification process, the thin-plate spline was computed and used to resample the voxelated atlas into the space defined by the model brain. The result is a canonical atlas aligned with the model MRI anatomy, and these two volumetric data sets are ready to serve as a target in the ANIMAL registration and segmentation procedure.

In summary, the steps involved in customizing the atlas for a patient's MRI are:

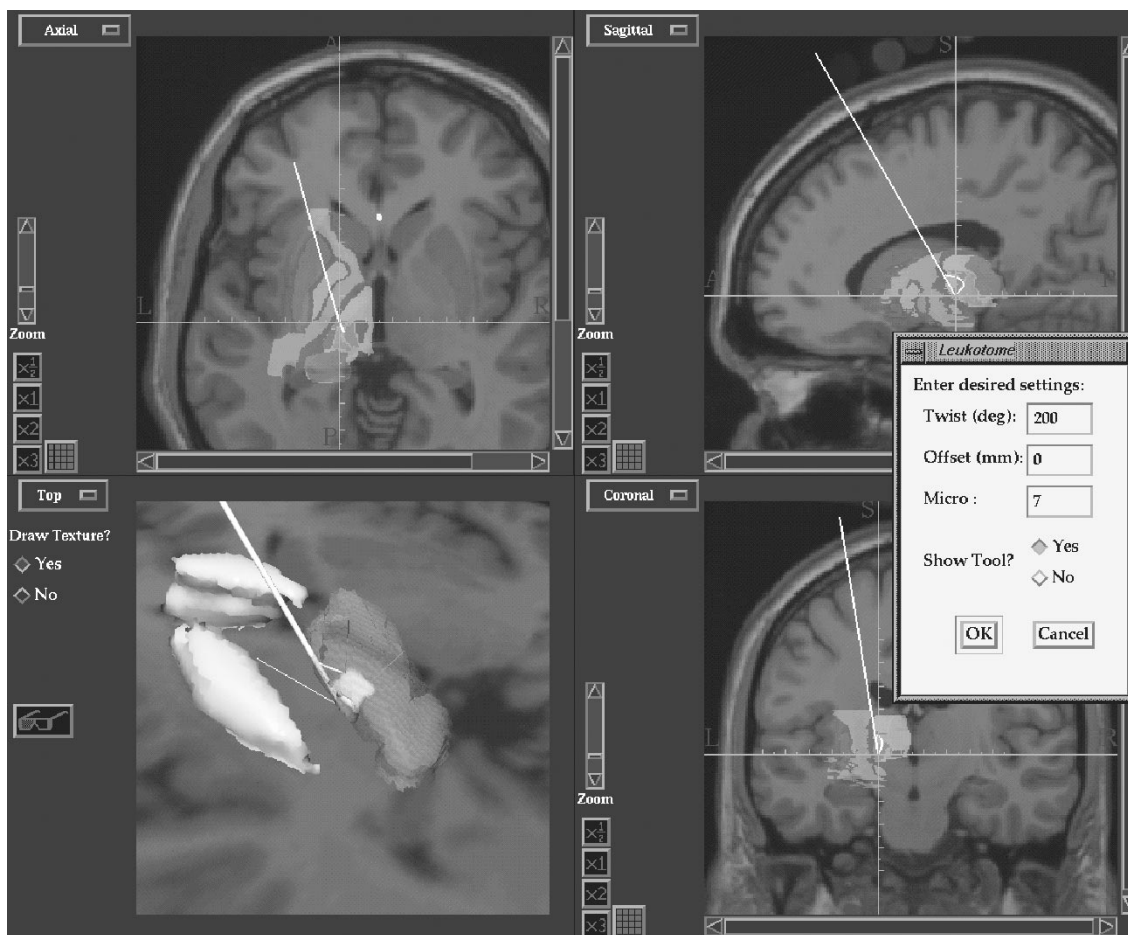


Fig. 7. The visualization platform. In the three 2-D views the atlas has been superimposed on the model brain. Projections of the leukotome onto the three standard planes can be seen in white. In the bottom left (3-D) view, surface-renderings of the putamen, caudate, thalamus (semitransparent), and the target Vim node in the thalamus can be seen, along with the leukotome and a texture map (MR intensity values) of the current axial slice for added anatomical context.

- automatic calculation of the nonlinear transformation from each patient’s MRI to the model MRI space using ANIMAL;
- deformation of the model-space (canonical) atlas onto the patient’s MRI space using the inverse of the nonlinear transformation.

D. Visualization Platform

The Image-guided Neurosurgery (IGNS) lab at the MNI has created a visualization platform, visual integration platform for enhanced reality (VIPER), for clinical applications. It is coded in C++ using two well-known and widely used libraries, namely Motif (Open Software Foundation) for the graphical user interface (GUI), and OpenGL (Silicon Graphics Inc., Mountain View, CA) for rendering-related tasks.

1) *2-D and 3-D Views*: The system is capable of superimposing (or merging) images from multiple sources such as MRI, CT, atlas slices, and functional/metabolic [positron emission tomography (PET) and functional magnetic resonance imaging (fMRI) and MR spectroscopy] modalities. The opacity (or relative blending) of the slices, as well as the window/level and color-map for each individual scan can be adjusted independently. In addition to the standard tri-planar views, two specific oblique views are also available.

- The “gun-view” orientation shows the plane perpendicular to a virtual probe that would be inserted in the patient’s head at a given declination and azimuth angle.
- An “ultrasound-view” (the plane that a 2-D ultrasound scanner would see), shows a user-defined plane containing the trajectory of the probe. This plane is usually chosen to include the stimulating probe and extended tip, or the leukotome shaft and cutting loop.

In addition, the 3-D structures of the volumetric atlas can be displayed as surfaces or meshes, using standard OpenGL primitives, again with independent colors and opacities, which is helpful in visualizing distinct nodes such as the relationship between different thalamic nuclei, the internal capsule and surgical instruments (Fig. 7). The images in the 2-D and 3-D windows are displayed in the same coordinate system, and points defined in the 3-D view can be tracked in the three orthogonal planes of the 2-D view. In the 3-D view, the objects can be manipulated interactively, enabling the user to rotate, translate, and zoom as desired.

2) *Virtual Neurosurgical Tools*: In order to represent neurosurgical tools in the interactive imaging environment, the stimulating electrode and the leukotome were accurately modeled (Fig. 3). In the case of the stimulator, the position of its tip was recorded over the 14 millimeters of its curvilinear

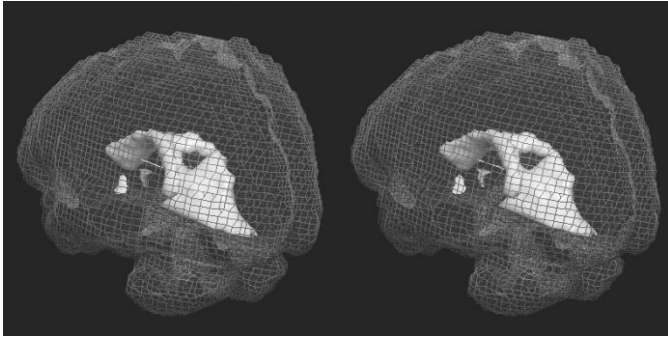


Fig. 8. Stereoscopic image pair showing a surface-rendering of a cerebral ventricle inside a mesh model of the cortex. The images are arranged for cross-eye viewing.

trajectory. For the leukotome, samples of the distance between the metallic wire and the shaft were measured at one millimeter intervals, and this measurement was repeated for all seven different settings (protrusions) of the leukotome loop. Such representations of the neurosurgical tools allow them to be displayed at all their possible settings in the 2-D and 3-D windows. The position of the target point (the tip of the curvilinear stimulator or the leukotome shaft) and the two angles of entry (declination and azimuth) can be specified in the native MRI coordinate system, or more commonly, in the coordinate system of the stereotactic frame. The user may place the virtual leukotome or stimulator anywhere in the volume of the coregistered atlas and MRI data set, allowing for both preoperative and intraoperative interactive planning and guidance. Note that in the standard 2-D views an orthogonal projection of the complete tool is displayed, rather than simply the points where the shaft intersects the 2-D (sagittal, coronal, or axial) plane. In the 3-D view however, the leukotome and stimulator are modeled as 3-D objects, allowing the user to fully appreciate their relationship to targets and surrounding areas.

3) *Stereoscopic Viewing*: Many of the monocular depth cues such as perspective, shading, occultation, and texture (i.e., mapping the original MRI intensity values onto selected planes as a context cue) have been incorporated into the 3-D view. However, one of the strongest short-range depth cues is stereopsis, which relies on binocular vision [22]. In order to make full use of the depth perception capabilities of the human visual system, VIPER is capable of displaying pairs of images in stereo. These images are rendered from two slightly different viewpoints (7° apart), simulating the left-eye and right-eye views of the 3-D objects (Fig. 8). The images are displayed on the computer monitor in a time-multiplexed fashion, such that the right and left views are alternated. Stereoscopic viewing is then enabled using a pair of CrystalEyes (StereoGraphics Corp., San Raphael, CA) shuttered eyewear, synchronized through an infrared emitter to the monitor's refresh rate, such that the right-eye and left-eye images are presented at the appropriate times [3], [23]. In the stereoscopic mode, the user is still able to manipulate the 3-D objects, and the control panel for the leukotome is also available, so that it may be rotated and translated as described earlier.

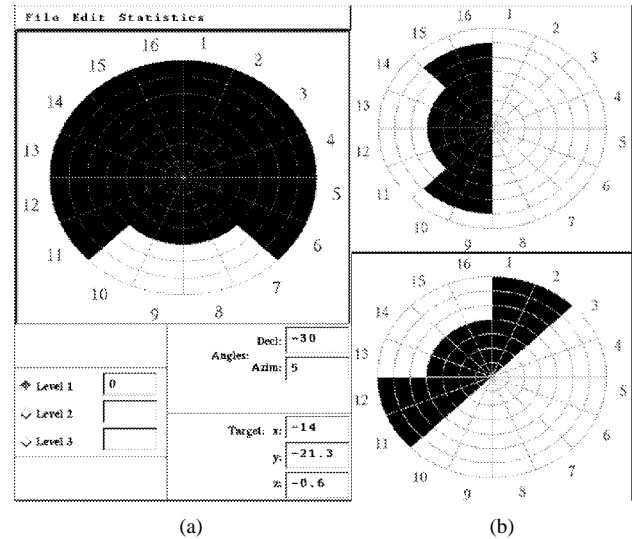


Fig. 9. (a) The lesion modeling graphical interface, along with (b) two other examples of other possible excision maps.

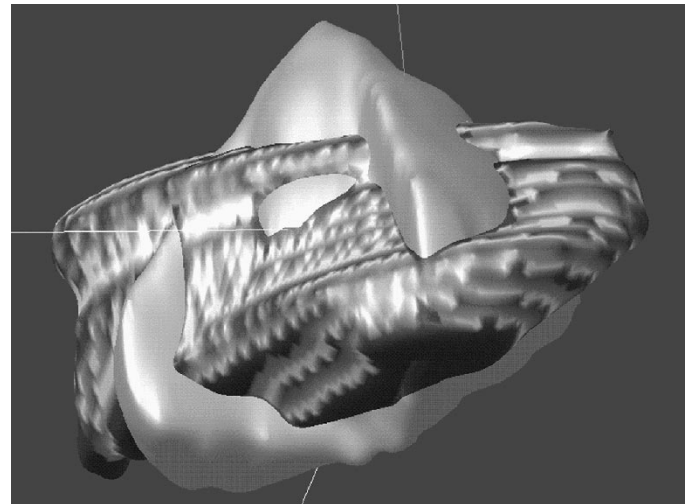


Fig. 10. A 3-D view of a virtual lesion (flat gray) of the right Gpm (textured gray).

4) *Lesion Modeling*: In addition to the visualization platform described, we created a graphical interface to allow the user to readily define potential volumetric lesions. This interface is presented in the shape of a dart-board divided into 16 sectors (Fig. 9), allowing the user to prescribe lesions of different size and shape by varying the leukotome protrusion setting at each sector. This prescription may be repeated at multiple leukotome positions, allowing for modeling of compound lesions. The user can visualize the virtual lesion on the VIPER platform either as a tomographic volume or as a 3-D surface-rendered object. It can then be compared to the atlas to ensure that no part of the virtual lesion overlaps critical structures (Fig. 10), and that the target volume is adequately covered.

III. RESULTS AND DISCUSSION

At the time of writing, this visualization platform has been employed in over 30 procedures. At this stage, this

system is used as an investigational tool only, and always in conjunction with the standard procedures and tools for these operations (e.g., ventriculography, intraoperative X rays, stimulation studies, etc.). In the majority of procedures, adequate atlas integration was obtained as validated by visual inspection, and physiological verification of the position of structures such as the internal capsule, the sensory thalamus, and the optic tract. Even though certain parts of the overall procedure have been well studied, we are in the process of conducting a more formal validation of the system by retrospective evaluation of the quality of atlas-MRI registration, and by correlating stimulus-response characteristics with respect to anatomical structures. Although the transformation of the native MRI into frame coordinates through identification of MRI-visible markers in stereotactic neurosurgery has an accuracy of 1–2 mm [4], [24], [25], the geometrical artifacts due to field inhomogeneity are highly dependent on the imaging parameters and can lead to distortions of up to 5 mm if no precautions are taken [26], [27]. At present, atlas registration is confirmed with physiological evidence in each case.

The accuracy of the ANIMAL algorithm has been previously evaluated for cortical and subcortical structures [18]. Typical misregistrations of well-defined structures in the subcortical areas of interest (e.g., putamen, head of the caudate nucleus) between the model brain and a patient MRI after registration using ANIMAL is 0.1–1.2 mm, with the larger errors generally being at sites on the periphery of the region of interest. In our current system, more than 250 point pairs were used to map only 16 structures between the atlas of cryogenic slices and the high-resolution low-noise model MRI. While less than ideal, since errors in the tagging process are carried over into the atlas registration, the landmark tagging and thin-plate spline procedure was used as a preliminary method of atlas definition, and was deemed to be a major improvement over the alternative of manually correlating atlas structures with patient MR images. We are currently working on a new voxelated atlas based on a database that is more detailed than the Schaltenbrand and Wahren atlas, to allow more precise registration between the atlas and model MRI.

The model MRI is a fundamental element in the success of many of the steps necessary in warping the atlas to a patient's MRI. The low noise in the model data set results in improved recognition of image-based landmarks which simplifies the manual tagging of homologous atlas/MRI points. It is important to note that of the four steps in creating an individualized atlas, only the last two (which require no intervention from a specialist) must be performed for every clinical case. In this regard, the labor-intensive manual tagging of the atlas to the model brain need be performed only once, and only the computationally expensive process of warping the model to the patient's MRI must be repeated for each patient.

The type of visual information that is available in the 2-D display panels is often a limiting factor. The fact that only slices through the volume can be visualized rather than complete 3-D structures, forces the neurosurgeon to mentally extrapolate their extent outside the slice, which is often challenging. It is particularly difficult to reconstruct the overall shape, size, and orientation of a region of interest or of a

proposed lesion site. Furthermore, the position of the surgical tools with respect to deep brain structures may be difficult to imagine especially when arbitrary trajectories are employed. The 3-D characteristics of VIPER were implemented to compensate for these inherent limitations of 2-D visualization, allowing greater insight into the global geometry of objects of interest. The 3-D views have facilitated the visualization of the operative tools and virtual lesions with respect to anatomical structures, a particularly important point since surgical tools may take different trajectories to their target structures in different cases.

IV. CONCLUSIONS

During functional stereotactic procedures, neurosurgical tools are inserted deep within critical subcortical areas. Since no craniotomy is performed, the neurosurgeon relies on indirect information obtained by imaging the brain with respect to a reference system. Furthermore, detailed parcellation of relevant targets necessary for functional neurosurgery is not visualized even with the best current imaging modalities. Since relatively arbitrary trajectories are taken to the target structure, the position of the neurosurgical tools and the configuration of the ultimate lesion must be mentally reconstructed. The procedure is further complicated by variations in individual anatomy, limiting the utility of standard reference atlases. We have described a system, that automatically integrates stereotactic atlases into the patient's MR image space. Anatomical structures are displayed either on tri-planar 2-D MR-integrated slices or in a 3-D window as surface-rendered objects. The position and geometry of the stereotactic neurosurgical tools with respect to deep brain structures may also be displayed on the 2-D slices, as well as in the 3-D window. While conventional methods provide sufficient anatomical information and precision for functional neurosurgical procedures such as thalamotomies or pallidotomies, the system described here 1) enhances the neurosurgeon's ability to reconstruct the geometry of critical structures in 3-D, 2) allows interactive intraoperative correlation of the results of physiological recording or stimulation with respect to the patient's anatomy, and 3) allows for generation of tailored lesions which conform to the target structure and avoid unnecessary encroachment upon neighboring brain nuclei or white matter tracts. From our initial experience, we believe that the system is very useful as an adjunct to performing a complex neurosurgical navigation task, enhances neurosurgical confidence in the quality of the anatomical and physiological stereotactic data base, reduces the probability of hemorrhagic complications by helping to limit the number of trajectories required for physiological confirmation, and improves surgical results by allowing for more limited lesions that conform to the target area.

We are extending the utility of the system to include a comprehensive record of stimuli and responses elicited during functional neurosurgical procedures, allowing us to create a physiological volumetric atlas which will serve as an additional neurosurgical tool and enhance understanding of brain function. VIPER is currently being enhanced to

incorporate modeling of lesions created with RF probes, in addition to the leukotome. Also, while target planning involving vessel avoidance is currently achieved using a simple stereotactic planning system that matches stereoscopic DSA images with the 3-D MRI, future enhancements to VIPER will include vascular information in the form of 3-D MR angiograms integrated with the MRI data [28].

The system has wide-ranging implications beyond stereotactic neurosurgery. We are also using it to evaluate the position of pathological lesions or areas of functional activation on PET and fMRI, with respect to subcortical structures within the basal ganglia or thalamus.

ACKNOWLEDGMENT

The authors wish to thank Dr. N. Kabani for her invaluable help in tagging the anatomical atlas to the model MRI, Dr. C. Holmes for helpful discussions and the use of the model MRI data set, and Dr A. Parrent, K. Finnis, M. Cyr and R. Comeau for their support and input.

REFERENCES

- [1] K. J. Burchiel, "Thalamotomy for movement disorders," [Review] [95 refs] *Neurosurg Clin. N Amer.*, vol. 6, pp. 55–71, Jan. 1995.
- [2] O. A. and Bertrand G., "Stereotaxic device for percutaneous twist-drill insertions of depth electrodes and for brain biopsy," *J. Neurosurg.*, vol. 56, pp. 307–308, 1982.
- [3] T. M. Peters, C. J. Henri, P. Munger, A. M. Takahashi, A. C. Evans, B. Davey, and A. Oliver, "Integration of stereoscopic DSA and 3-D MRI for image-guided neurosurgery," *Computerized Med. Imag., Graphics*, vol. 18, pp. 289–299, 1994.
- [4] P. Munger, "Accuracy considerations in MR image-guided neurosurgery 1994," masters thesis, McGill Univ., Montreal, P.Q., Canada.
- [5] R. L. Alterman, B. A. Kall, H. Cohen, and P. J. Kelly, "Stereotactic ventrolateral thalamotomy: Is ventriculography necessary?," *Neurosurg.*, vol. 37, pp. 717–721, Oct. 1995.
- [6] S. Obrador, "A simplified neurosurgical technique for approaching and damaging the region of the globus pallidus in Parkinson's disease," *J. Neurol Neurosurg. Psychiatry*, vol. 20, 1957.
- [7] G. Bertrand, H. Jasper, A. Wong, and G. Mathews, "Microelectrode recording during stereotactic surgery," *Clin. Neurosurg.*, vol. 16, pp. 328–355, 1969.
- [8] F. H. Tomlinson, C. R. Jack Jr., and P. J. Kelly, "Sequential magnetic resonance imaging following stereotactic radiofrequency ventralis lateralis thalamotomy," *Neurosurg.*, vol. 74, pp. 579–584, 1991.
- [9] A. L. Benabid, P. Pollak, D. Gao, D. Hoffmann, P. Limousin, E. Gay, I. Payan, and A. Benazzouz, "Chronic electrical stimulation of the ventralis intermedialis nucleus of the thalamus as a treatment of movement disorders," *J. Neurosurg.*, vol. 84, pp. 203–214, Feb. 1996.
- [10] J. Talairach and P. Tournoux, *Co-Planar Stereotaxic Atlas of the Human Brain*. Stuttgart, Germany: Georg Thieme Verlag, 1988.
- [11] ———, *Referentially Oriented Cerebral MRI Anatomy*. Stuttgart, Germany: Georg Thieme Verlag, 1993.
- [12] G. Schaltenbrand and P. Wahren, *Introduction to Stereotaxis with an Atlas of the Human Brain*. Stuttgart, Germany: Thieme, 1977.
- [13] W. L. Nowinski, A. Fang, B. T. Nguyen, J. K. Raphael, L. Jagannathan, R. Raghavan, R. N. Bryan, and G. A. Miller, "Multiple brain atlas database and atlas-based neuroimaging system," *Comput. Aided Surg.*, vol. 2, pp. 42–66, 1998.
- [14] U. Tiede, M. Bomans, K. H. Hoehne, A. Pommert, M. Reimer, T. Schiemann, and W. Lierse, "A computerized three-dimensional atlas of the human skull and brain," *Amer. J. Neuroradiol.*, vol. 14, pp. 551–559, 1993.
- [15] G. Bertrand, A. Oliver, and C. J. Thompson, "The computerized brain atlas: Its use in stereotaxic surgery," *Trans. Amer. Neurol. Assoc.*, vol. 98, pp. 233–237, 1973.
- [16] C. J. Thompson and G. Bertrand, "A computer program to aid the neurosurgeon to locate probes used during stereotaxic surgery on deep cerebral structures," *Comput. Programs Biomed.*, vol. 2, pp. 265–276, Nov. 1972.
- [17] J. D. Foley, A. van Dam, S. K. Feiner, and J. F. Hughes, "Computer graphics, principles, and practice." Reading, MA: Addison-Wesley, 1990.
- [18] D. L. Collins, T. M. Peters, and A. C. Evans, "An automated 3-D nonlinear image deformation procedure for determination of gross morphometric variability in the human brain," in *Proc. 3rd Conf. Visualization in Biomedical Computing*, (VBC-III), SPIE, vol. 2359, Seattle WA, R. A. Robb, Ed., 1994, pp. 180–190.
- [19] C. J. Holmes, R. Hoge, D. L. Collins, R. Woods, A. W. Toga, and A. C. Evans, "Enhancement of MR images using registration for signal averaging," *J. Comput. Assist. Tomogr.*, vol. 22, pp. 324–333, 1998.
- [20] R. Henkelman, "Measurement of signal intensities in the presence of noise in MR images," *Med. Phys.*, vol. 12, pp. 232–233, 1985.
- [21] F. L. Bookstein, "Principal warps: Thin-plane splines and the decomposition of deformations," *IEEE Trans. Pattern Anal. Machine Intell.*, vol. 11, pp. 567–585, 1989.
- [22] R. Patterson, *Human Stereopsis Human Factors*, vol. 36, pp. 669–692, 1998.
- [23] T. M. Peters, B. L. K. Davey, P. Munger, R. Comeau, A. C. Evans, and A. Olivier, "Three-dimensional multimodal image-guidance for neurosurgery," *IEEE Trans. Med. Imag.*, vol. 15, pp. 121–128, 1996.
- [24] T. M. Peters, J. A. Clark, G. B. Pike, C. J. Henri, D. L. Collins, D. Leksell, and O. Jeppsson, "Stereotactic neurosurgery planning on a personal-computer based workstation," *J. Digital Imag.*, vol. 2, pp. 75–81, 1989.
- [25] R. L. Galloway Jr., R. J. Maciunas, and J. W. Latimer, "The accuracies of four stereotactic frame systems: An independent assessment," *Biomed. Instrum., Technol.*, vol. 25, pp. 457–460, 1991.
- [26] A. Gauvin, "Geometrical distortion of magnetic resonance images 1998," masters thesis, McGill Univ., Montreal, P.Q., Canada, 1998.
- [27] T. S. Sumanaweera, J. R. Adler, G. H. Glover, P. F. Hemler, P. A. van den Elsen, D. Martin, and S. Napel, "Method for correcting magnetic resonance image distortion for frame-based stereotactic surgery, with preliminary results," *J. Image Guid. Surg.*, vol. 1, pp. 151–157, 1995.
- [28] T. M. Peters and G. B. Pike, "Magnetic resonance angiography in image-guided surgery," in *Advanced Neurosurgical Navigation*, Maciunas R. and E. Alexander, Eds. New York: Thieme Medical, 1998.